Modeling of the Phase Noise in Space Communication Systems

Ondřej BARAN, Miroslav KASAL

Dept. of Radio Electronics, Brno University of Technology, Purkyňova 118, 612 00 Brno, Czech Republic

xbaran03@stud.feec.vutbr.cz, kasal@feec.vutbr.cz

Abstract. *Our work is focused on the investigation of an influence of an additive thermal noise and a multiplicative phase noise in space communication chains. The most important properties of both noise types are summarized. The main concern of this paper is on the multiplicative phase noise that is especially important in systems with the phase shift keying. The simulation procedure for modeling of a signal degraded by the multiplicative phase noise is described. One starts from the frequency domain, where noise properties are set up. Five basic phase noise types can be included. After a passing to the time domain, the final noisy signal is obtained. To prove the modeling correctness, two ways are used. Firstly, Allan variances are utilized as a time domain processing. Finally, for a comparison, the direct conversion formula from the frequency to the time domain is exploited. Created signal corrupted by the phase noise expresses the harmonic oscillator output signal. A pair of these oscillators, disturbed by different phase noise processes, is installed into a communication channel model and with its help, the simultaneous influence of both oscillators on the useful signal is examined. Results show a good coincidence with theoretical presumptions.*

Keywords

Multiplicative phase noise, additive thermal noise, frequency stability, oscillator, Allan variances.

1. Introduction

Many negative factors affect and limit possibilities of space communication chains. Data rates, communication distances, the velocity of communicating objects connected with the Doppler frequency shift and the noise belong among the most severe factors. Indeed, both noise forms, the additive noise and the multiplicative noise, respectively, corrupt the original signal. While the additive thermal noise arises only from the receiver side of the communication system, the multiplicative phase noise is projected from the receiver side local oscillators as well as from the transmitter side carrier sources. A question of the frequency stability is closely connected with the phase noise. Deep space communication links utilize the PSK modulation that, first of all, gives the best BER with the minimum power consumption and it is easy to implement to the system. The sub-carriers are often used to minimize the influence of the main carrier phase noise [1], [2], [3].

The simulation procedure including both noise types is being developed. This procedure counts with the phase noise of all oscillators on both sides of the communication chain as well as with the additive thermal noise related to the receiver side of the communication system.

2. Description of the Communication System under Simulations

Current approaches count with the presence of the additive thermal noise and the multiplicative phase noise separately. Some of them solve the additive noise related to the receiver side [4], other studies follow the properties and the influence of the multiplicative phase noise of the oscillator [5], [6]. The aim of our work is to include an influence of both noise types in the area of long distance space communications. Here, one decreases the system bandwidth to eliminate the influence of the additive thermal noise. By this way, a higher SNR is obtained. But the bandwidth decrease brings one closer to the vicinity of the carrier, where the amount of the multiplicative phase noise is increasing. The proposed model of the communication system is going to include both noise types. The effort is to cover the influence of bandwidth changes on SNR at the presence of the additive thermal noise as well as the multiplicative phase noise.

Fig. 1 shows a block diagram of the simplified communication system that shapes the base for simulations. All blocks are ideal except two oscillators (one in the transmitter and the other in the receiver) corrupted by the phase noise and except the transmission channel that is modeled as an AWGN channel. The additive noise contributors on the receiver side are recalculated to a place of a receiving antenna and are combined with the channel noise. Thus, all of the additive thermal noise is included in the signal to thermal noise ratio, which is the main parameter characterizing the AWGN channel.
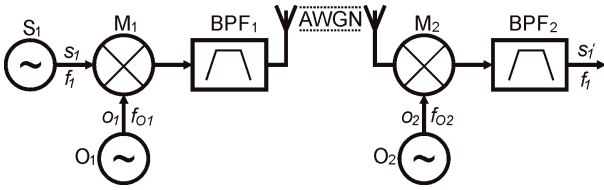
Fig. 1. The simplified block diagram of the simulated communication system.

A source S_1 generates a pure harmonic signal s_1 with a frequency f_1. This is the useful signal that is being transmitted through the system. The multiplicative phase noise degrades a signal o_1 of a transmitter local oscillator O_1. This is utilized for the useful signal s_1 mixing in a mixer M_1. It causes the frequency transposition of the signal s_1 from its base band to the RF band in the vicinity of the carrier o_1. The proper part of the mixer output is chosen by the band-pass filter BPF_1. At this time, the signal is transmitted by the antenna through the AWGN channel towards the receiver. In the channel, the transmitted signal is corrupted by the additive thermal noise. The received signal is mixed in a mixer M_2 with a help of a receiver local oscillator O_2 to the base band. Unwanted mixing products are suppressed in the band-pass filter BPF_2. The signal s_1' in the base band leads to the demodulator and other blocks for further processing. The signal o_2 of the oscillator O_2 is also corrupted by the multiplicative phase noise.

The bandwidth of the BPF_2 on the receiver part of the system also affects the amount of the noise. Thus, it determines the carrier to noise ratio before the demodulator and in the dependency on the modulation, the signal to noise ratio after the demodulator.

Following paragraphs summarize the most important features of both noise types. The main concern is on the multiplicative phase noise and thus, the way of its implementing to the simulation model is showed. The additive thermal noise with the white Gaussian distribution implies from the transmission channel as well as from the receiver side of the system. Sky and ground contribute to the transmission channel thermal noise. Parameters of the noise are related to the ambient and they can't be affected. Thus, only the proper choice of receiver components can hold the overall receiver thermal noise as low as possible. The multiplicative phase noise rises from oscillators implemented in the whole system.

3. Thermal Noise and AWGN

The thermal noise is the most widespread noise form that can be found in electronic circuits and systems. This noise mechanism arises from resistive parts that are always presented in all electronic circuits. Resistive materials with the certain temperature produce the certain voltage fluctuations on their terminals. These fluctuations are caused by randomly moving free electrons that are forced by their thermal energy that is proportional to the temperature. The thermal noise amplitudes can be statistically described by the Gaussian distribution. The mean square noise voltage $\overline{v_n^2}$ [4], [7] can be obtained by

$$\overline{v_n^2} = 4kTBR \tag{1}$$

where k is the Boltzmann's constant, R is a value of the resistance with the thermodynamic temperature T. B represents the noise bandwidth [7]. A noise power spectral density describes a noise power concentrated in the unity noise bandwidth B. The thermal noise power spectral density has a flat course according to the relation [7]

$$N_0 = kT. \tag{2}$$

In the time domain, the thermal noise, denoted as $n(t)$, can be simply added to the useful band pass signal as the following equation describes on the basic example with a real harmonic signal

$$s(t) = A \cdot \sin(2\pi f t + \varphi_0) + n(t). \tag{3}$$

The harmonic signal is characterized by its amplitude A, instantaneous frequency f and initial phase φ_0. All these quantities are independent on the time t. Exactly the t dependent term $n(t)$ brings the thermal noise to the useful signal. From this point of view, a thermal noise is modeled as an additive white Gaussian noise (AWGN).

Every block of the receiver chain consists of resistive parts producing the thermal noise. Two equivalent ways of describing the thermal noise influence can be used, a noise figure or an equivalent noise temperature, respectively.

The noise factor F shows, how the certain block degrades the signal to noise ratio SNR. The noise factor is characterized at a certain input frequency as the ratio of the input SNR to the output SNR [8]. The noise temperature T is connected with the noise factor according to the following term

$$T = T_0(F - 1), \tag{4}$$

where T_0 is the real thermodynamic temperature of the noise source [8], [9]. With a help of the noise temperature, one can model a noisy part of the system as a noise-free block supplied by the resistor with the equivalent noise temperature T, which causes the appropriate noise power at the output of the whole part [9].

From the whole communication system point of view, as was mentioned earlier, one considers that the thermal noise is projected only on the receiver side of this system. In this case, one can aim only to the receiver part of the system, see Fig. 2. The receiver usually consists of an antenna with the low noise preamplifier connected the nearest place to the antenna. Consequently, the signal is led through the transmission line (coaxial cable) to the mixer M_R, where the signal gets from the radio frequency band to the intermediate frequency band. After the filtration in the band-pass filter BPF_R, the signal is led to the receiver. All these parts are sources of the thermal noise, which can be

described by the noise factor F or by the equivalent noise temperature T, respectively (appropriate quantities are described directly in Fig. 2).
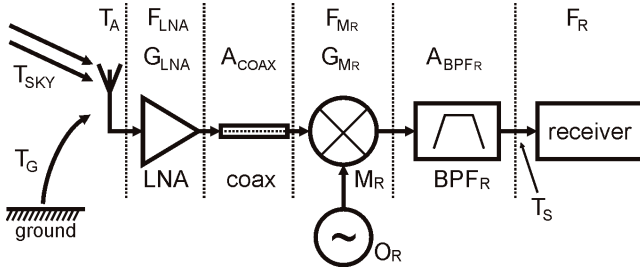

Fig. 2. The detailed block diagram of the system receiver part.

To express the thermal noise influence of the whole receiver part, the quantity of a system noise temperature T_S is introduced

$$T_S = \frac{G_{LNA}G_{MR}}{A_{COAX}A_{BPFR}}\left[T_A + T_0(F_{LNA}-1)\right]+$$
$$+\frac{G_{MR}}{A_{COAX}A_{BPFR}}T_0(A_{COAX}-1)+ \quad (5)$$
$$+\frac{G_{MR}}{A_{BPFR}}T_0(F_{MR}-1)+$$
$$+\frac{T_0(A_{BPFR}-1)}{A_{BPFR}}+T_0(F_R-1).$$

According to the Friis's formula for noise [8], [9] the total noise figure of the subsystem LNA-COAX-M_R-BPF_R-receiver related to the antenna connector is calculated. The total noise figure is transformed to the total noise temperature (4) and consequently, the antenna noise temperature T_A is added. This expression is divided by the overall attenuation of the subsystem LNA-COAX-M_R-BPF_R-receiver. The result is the system noise temperature T_S (5). Noise figures of passive components are directly equal to their power attenuation [9].

As it is depicted in Fig. 2, T_S is related to the input port of the receiver and it expresses the necessary increment of the temperature of the inner generator conductance, related to the reference temperature T_0, to obtain the same noise power at the receiver output, as the real noisy part were replaced by their noise-free equivalents. In the area of space communications, where one considers the signal reception from space probes and satellites, the antenna is pointed to the cold sky with a brightness temperature T_{SKY}. A final noise temperature of the antenna T_A is given by a sum of T_{SKY} and by the contribution of the Earth noise temperature T_G, which is dependent on an antenna elevation angle [9].

The system noise temperature expresses the amount of the noise at the input of the receiver. Exactly at this point, the total calculated noise can be added to the useful transmitted signal. Thus, the model of the transmission channel affected by the thermal noise can be obtained, as can be seen on the simplified block diagram in Fig. 3.
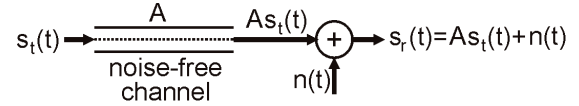

Fig. 3. The noise model of the receiver part.

In the time domain, this procedure is described by an equation

$$s_r(t) = A \cdot s_t(t) + n(t) \quad (6)$$

where the $s_t(t)$ is a useful transmitted signal. Factor A is a noise-free channel attenuation. $n(t)$ expresses the total noise recalculated to the point of its addition (see Fig. 3). $s_r(t)$ is the final signal presented on the receiver input port degraded by the noise.

4. Phase Noise

In the following paragraphs, the term phase noise is described. The phase noise is directly connected with the stability of frequency generators – oscillators. In the area of high frequency space communications, the harmonic oscillators are mostly used. Because of the oscillator output amplitude regulation ability and the output signal limitation possibility, the amplitude is considered constant through the time and the additive amplitude noise can be neglected [5]. For the simplicity, after the amplitude normalization to unity, the oscillator output signal can be described by the equation

$$u(t) = 1 \cdot \sin(2\pi f_0 t + \varphi(t)). \quad (7)$$

f_0 represents the nominal frequency – the carrier. From (7) it implies, that the instantaneous phase $\varphi(t)$ is the only parameter containing the noise. In a case of sufficiently small phase fluctuations $\varphi(t)$, the equation (7) expresses the narrow-band phase modulated signal [10], [11].

4.1 Basic Terms and Expressions

Stability measurements utilize the method of a comparison between the measured oscillator and a reference source. The reference needs at least the higher-order stability than the measured signal source. For other purposes, the reference is considered as an ideal harmonic source with the zero noise term $\varphi(t)$ in (7).

A fractional frequency $y(t)$ and time fluctuations $x(t)$, respectively, are very helpful quantities used for the stability analysis. The fractional frequency can be obtained by comparing the measured oscillator with the reference according to

$$y(t) = \frac{f(t)-f_0}{f_0} = \frac{1}{2\pi f_0}\frac{d\varphi}{dt} = \frac{dx}{dt} \quad (8)$$

where $f(t)$ represents the time variant frequency of the measured oscillator. Phase fluctuations $\varphi(t)$ are related to time fluctuations $x(t)$ by the term $\varphi(t)=2\pi f_0 \cdot x(t)$ [10], [12].

The evaluation of the oscillator noise behavior can be achieved either in the frequency domain or in the time domain. Each expression has its advantages and disadvantages. The parameter, according to which the domain is chosen, is the time of the measuring. The short time frequency stability is examined in the frequency domain for the short measuring time, less than 1 second. While, for the longer measuring time, more than 1 second, the time domain is used for the long time frequency stability investigation.

The most common and transparent quantity expressing the frequency stability in the frequency domain is directly denoted as the phase noise. It is equal to the ratio of the noise power measured in a 1 Hz noise bandwidth located on the specific offset frequency f from the carrier to the power of the useful signal, the carrier [5], [8]. With a help of the fractional frequency $y(t)$, the spectral density of frequency fluctuations $S_y(f)$ can be calculated and consequently the phase noise $L(f)$ can be obtained according to

$$L(f) = 10 \cdot \log\left(\frac{1}{2}\left(\frac{f_0}{f}\right)^2 S_y(f)\right) =$$
$$= 10 \cdot \log\left(\frac{1}{2}S_\varphi(f)\right) . \tag{9}$$

A term $S_\varphi(f)$ denotes the spectral density of phase fluctuations. Real courses of three previously mentioned quantities can be divided into several asymptotic parts that refer to appropriate noise characters. They are mathematically expressed with a help of a power law. Slopes of asymptotes in the log-log graphical representation are described by the powers α and β of the power law. The following equation (10) describes asymptotic representations of $S_y(f)$ and $S_\varphi(f)$, respectively [10] (according to (9), these expressions are equivalent) .

$$S_y(f) = h(\alpha)f^\alpha \text{ and } S_\varphi(f) = h(\beta)f^\beta . \tag{10}$$

Transfer functions $h(\alpha)$ and $h(\beta)$ are related to proper powers, α or β, respectively. Tab. 1 below summarizes five basic phase noise processes and corresponding powers (for a comparison, powers μ for the time domain representation are also mentioned).

In the time domain, the noise, represented by the time dependent time fluctuations or fractional frequency fluctuations (8), is processed statistically. The independent variable τ denotes the averaging time and it is derived from the fundamental sampling period τ_0 according to

$$\tau = m \cdot \tau_0 \tag{11}$$

where integer m represents an averaging factor. With a help of τ, the basic measure for the frequency stability expression is the two-sample Allan variance $\sigma_y^2(\tau)$ [10]. While the standard variance diverges for the flicker noise, the Allan variance is convergent for all basic noise processes (shown in Tab. 1), [10].

Noise Characters	Asymptotes Powers			
	$S_y(f)$	$S_\varphi(f)$	$\sigma_y^2(\tau)$	Mod $\sigma_y^2(\tau)$
	α	β	μ	μ
white PM	2	0	-2	-3
flicker PM	1	-1	-2	-2
white FM	0	-2	-1	-1
flicker FM	-1	-3	0	0
random walk FM	-2	-4	1	1

Tab. 1. Powers of power law decompositions of stability measures for basic noise processes.

Several types of Allan variances are established for the oscillatory system stability examination [10]. A two-sample simple Allan variance is the most common method and can be calculated according to (12). Its biggest advantage is the lowest computational severity, but its confidence interval isn't very good [10]. Thus, for the longer averaging period τ, the course is quite curly. Another possibility is the overlapping Allan variance (13), which extends the degree of freedom, the confidence interval is much better and the course is smoother [10]. The increased computational power demands pay for this improvement.

$$\sigma_y^2(\tau) = \frac{1}{2(N-2)\tau^2} \sum_{i=1}^{N-2}(x_{i+2} - 2x_{i+1} + x_i)^2 \tag{12}$$

$$\sigma_y^2(\tau) = \frac{1}{2(N-2m)\tau^2} \sum_{i=1}^{N-2m}(x_{i+2m} - 2x_{i+m} + x_i)^2 \tag{13}$$

These two variances are not capable of distinguishing between white and flicker noise types. For this reason, additional averaging is implemented in the modified Allan variance [10]

$$Mod\ \sigma_y^2(\tau) = \frac{1}{2m^2\tau^2(N-3m+1)} \cdot$$
$$\cdot \sum_{j=1}^{N-3m+1}\left\{\sum_{i=j}^{j+m-1}(x_{i+2m} - 2x_{i+m} + x_i)\right\}^2 . \tag{14}$$

The final course of τ dependent Allan variance σ_y^2 can be also depicted in a log-log plot, where the asymptotic parts corresponding to the individual noise processes can be observed. Slopes of asymptotes are equivalent with powers μ of the $\sigma_y^2(\tau)$ course spreading according to the power law

$$\sigma_y^2(\tau) = h(\mu)\tau^\mu \tag{15}$$

where $h(\mu)$ presents the μ dependent transfer function [10].

Tab. 1 connects basic noise processes with powers μ in the time domain and with powers α and β characterizing the frequency domain stability expressions. The following dependency [10] between all powers can be achieved

$$\mu = -\alpha - 1 = -\beta - 3 . \tag{16}$$

For recalculations between the frequency and the time domain, the direct conversion formula is derived. The general transfer equation for the Allan variance [10] has a form

$$\sigma_y^2(\tau) = \int_0^{f_h} S_y(f) \cdot |H(f)|^2 \, df \qquad (17)$$

where the symbol f_h means the upper cut off frequency of the measuring system and in this simulation case, it is equal to a half of the sampling frequency. $|H(f)|^2$ is the transfer function of the time domain sampling function.

Because of the presence of five independent noise processes (see Tab. 1), the calculation of the integral (17) can be spread into five independent parts and the result is the sum of these fractional calculations [10]

$$\sigma_y^2(\tau) = h_{-2} \cdot A \cdot \tau + h_{-1} \cdot B + h_0 \cdot C \cdot \tau^{-1} + \\ + h_1 \cdot D \cdot \tau^{-2} + h_2 \cdot E \cdot \tau^{-2}. \qquad (18)$$

Factors h_n define levels of certain noise characters in the frequency domain and constants A, B, C, D and E imply from the calculation of the integral (17) [10]. These constants are different for simple or overlapping Allan variances and for the modified Allan variance [12], [13]. Graphical representations (asymptotic courses as well as simulation results) are summarized in Section 5, where achieved results are discussed.

4.2 Phase Noise Implementation to Simulations

The main interest is to create a signal degraded by the phase noise with certain parameters. A progress chart (see Fig. 4) summarizes the following simulation description. The frequency domain is chosen as the starting point where one sets up the properties of the phase noise $L(f)$ – noise powers on appropriate offset frequencies. These properties can be obtained by measurements of real oscillators. In the measured real phase noise course, one can find parts corresponding to basic noise processes shown in Tab. 1. Other important simulation quantities are the carrier frequency f_0 and the simulation sampling frequency f_s. The course between given points is linearly interpolated and represents the asymptotic course of $L(f)$, where slopes of asymptotes directly refer to characteristic properties of the noise (according to Tab. 1). The noise power at the zero offset frequency is set up to 0 dBc/Hz, while at the most distant frequency from the carrier, the noise power has to be small but finite. The linearly interpolated vector of $L(f)$ is recalculated to the linear scale and randomized by the sample by sample multiplication with a unity power AWGN vector [11]. (AWGN function is used only as a tool for the randomization of the phase noise data in the frequency domain and it has nothing to do with the thermal noise description in Section 3.)

The random noise data are transformed from the frequency domain to the time domain with the help of IFFT.

Providing the small time dependent phase changes $\varphi(t)$, the narrow-band phase modulation can be supposed and after some mathematical modifications and simplifications of (7), one obtains (expecting initial sine wave, as in (7))

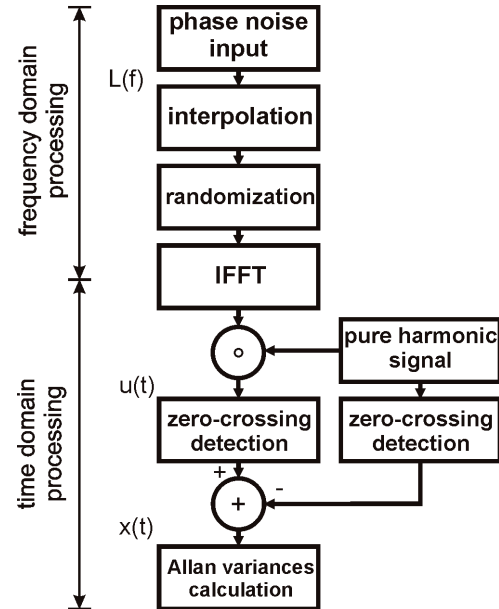$$u(t) \cong 1 \cdot [\sin(\omega_0 t) - \varphi(t) \cdot \cos(\omega_0 t)]. \qquad (19)$$

Fig. 4. The progress chart for the creation and verification of the signal degraded by a phase noise. (A mathematical operation denoted as ○ is described by the equation (19).)

From this point of view, the oscillator output signal disturbed by the phase noise with certain properties is created. To verify the correctness of the phase noise generation process, the time domain stability processing is used. This signal is compared with the reference that is also derived from (7), but the term $\varphi(t)$ is zero. Both signals zero-crossings are compared and time dependent time fluctuations $x(t)$ are obtained. If the exact zero-crossing isn't found, the linear interpolation from adjacent samples is used. Calculated time dependent time fluctuations are then processed statistically with a help of two-sample Allan variances according to equations (12), (13) and (14).

To cover the longest possible interval of τ and simultaneously, not to exceed the computational power and the memory, some restrictions are made. According to (11), the simple Allan variance utilizes the whole range of m to define τ. For computations of the overlapping Allan variance and the modified Allan variance, one takes only some m in each decade to get final τ according to (11).

For a verification of the simulation correctness, a direct domain conversion formula is used. According to (18), the interpolated asymptotic course $L(f)$ before the randomization in the frequency domain is directly recalculated to the time domain, where it represents the asymptotic course $\sigma_y^2(\tau)$. The verification is based on the graphical expressions as well as on the slopes of asymptotes obtained from the power law spreading.

5. Achieved Results

At the present, the multiplicative phase noise has been modeled and simulated, while presumptions shown in previous paragraphs are utilized. The simulation process is tested on the imaginary oscillator with the output frequency $f_O = 10$ MHz, the sampling frequency is set to $f_s = 100$ MHz. These parameters have been chosen as a compromise between the accuracy and the computational severity. The output frequency corresponds to the frequency of common frequency standards.

The imaginary oscillator output signal is degraded by the certain course of the phase noise described in the frequency domain. All five basic phase noise processes (see in Tab. 1) are implemented to simulations. The overall asymptotic phase noise course $L(f)$ is shown in Fig. 5. Fig. 6 depicts the corresponding course of time dependent time fluctuations $x(t)$ in the time domain.
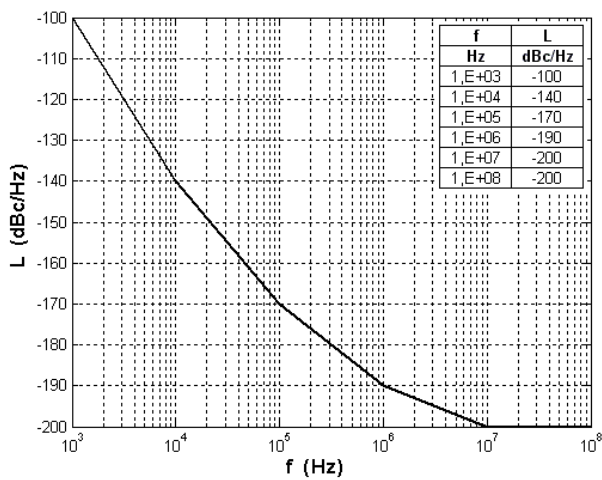

f	L
Hz	dBc/Hz
1,E+03	-100
1,E+04	-140
1,E+05	-170
1,E+06	-190
1,E+07	-200
1,E+08	-200

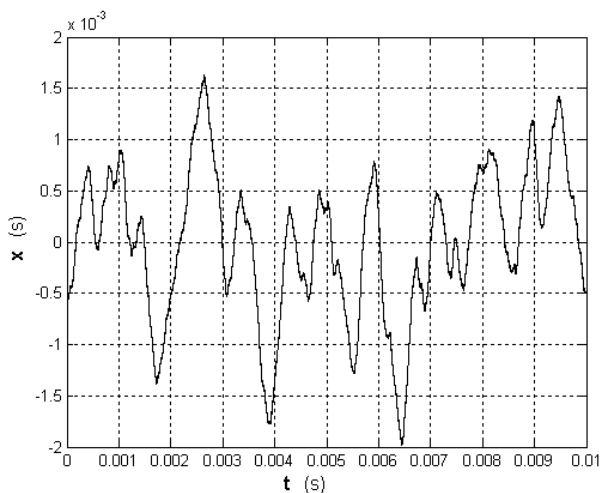**Fig. 5.** The asymptotic phase noise course $L(f)$ used for modeling.

Fig. 6. The section of time dependent time fluctuations $x(t)$ corresponding to $L(f)$ depicted in Fig. 5.

The resulting simulated signal degraded by the phase noise is examined in the time domain with a help of Allan variances. Firstly, simple and overlapping Allan variances

are used for the stability processing. Results implying from simulations are depicted in Fig. 7 and are compared with direct conversion asymptotes. Fig. 7 tries to cover a maximum influence of all phase noise characters, a range of averaging time τ is large and that's why Fig. 7 captures only the curve for the overlapping Allan variance. Due to the figure resolution, the overlapping Allan variance course is not distinguishable from simple Allan variance results. The white PM and the flicker PM noise characters aren't differentiated neither from the simulation results, nor from slopes of the direct conversion asymptotic course.
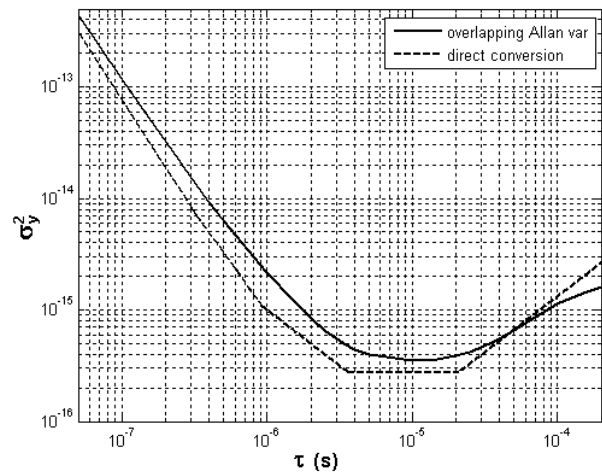

Fig. 7. The overlapping Allan variance course – simulated and direct conversion results.

Finally, to find the border between the white PM noise and the flicker PM noise, the modified Allan variance is utilized. Fig. 8 shows simulation results as well as the direct conversion asymptotic course.
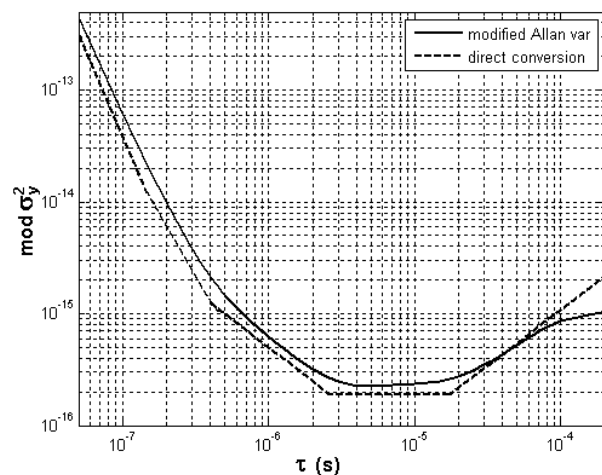

Fig. 8. The modified Allan variance course – simulated and direct conversion results.

Simulated results present a good agreement with the direct calculation. These results divert more only for the random walk FM noise part, which is related to the long averaging time τ. Deviations increase with the increasing averaging time τ. This can be caused by the decreasing number of samples that are used for a computation of the

longer averaging time. Another fact that can contribute to deviations ensues from the simulation procedure itself. The final noisy signal is composed of step by step created sections. Due to a periodical adding of these sections, some additional disturbing harmonic components can be presented in the time dependent time fluctuations course $x(t)$. This leads to the decreasing of Allan variance values for the random walk FM noise type. The phase noise model is going to be improved in our future work.

At this time, one can simulate an oscillator output signal disturbed by the arbitrary phase noise. It enables to model the whole space communication chain and to include all oscillators in it. The simplified block diagram depicted in Fig. 1 is modified. The transfer channel is considered to be ideal – noise free and lossless. Thus the additive thermal noise, as it was discussed in Section 3, is temporarily neglected and it is not taken into account in simulations.

Properties of individual parts describing the model in this paragraph imply from the primary settings serving for the verification of the simulation process and for the transparent representation of results. Parameters of blocks in the proposed model are following. The system sampling frequency $f_s = 100$ MHz. The transmitter side input source S_1 is represented by the sine harmonic signal s_1 with the frequency $f_1 = 100$ kHz and the noise floor 150 dB below the useful signal level. The transmitter local oscillator O_1 produces a sine wave with the frequency $f_{O1} = 10$ MHz and is disturbed by the white PM phase noise with a flat course on the level -150 dBc/Hz in a frequency range from 1 kHz to 50 MHz. After mixing in M_1, the upper harmonic component is selected by the band-pass filter BPF_1 with bandwidth ±30 kHz around $f_{O1}+f_1$. The receiver local oscillator signal o_2, a sine wave has the frequency $f_{O2} = 10$ MHz, is degraded by the random walk FM noise with an asymptote slope -40 dB/decade and is starting at the offset frequency 100 Hz with the level -100 dBc/Hz. Receiver down mixing harmonic products are filtrated in BPF_2 with the bandwidth ±80 kHz around f_1. Other components are ideal, both band-pass filters have ideal rectangular transfer functions and their bandwidths are chosen properly to demonstrate the phase noise influence.

Graphical results of individual oscillators O_1 and O_2 phase noise courses as well as of the phase noise influence in the output signal s_1' are depicted in the frequency domain in Fig. 9. The resultant SSB course of s_1' combines both oscillators phase noise and their influence is formed by the band-pass filters. From the carrier, up to the cut-off frequency of the BPF_1, the resultant noise course is equal to the vector summation of both oscillators phase noises. Between cut-off frequencies of the BPF_1 and BPF_2, the resultant noise course corresponds only with the phase noise of the local oscillator O_2. A vector summation of both oscillators phase noise contributions can be simply derived according to the signal passing through the simplified model and with a help of (7). After mathematical modifications, the system output signal is equal to

$$s_1' = a \cdot \sin\left(2\pi f_1 t + \varphi_{o1}(t) - \varphi_{o2}(t)\right) \qquad (20)$$

where a is the output signal amplitude. $\varphi_{o1}(t)$, $\varphi_{o2}(t)$ are time dependent phase fluctuations of both oscillators directly related to their phase noise [10].
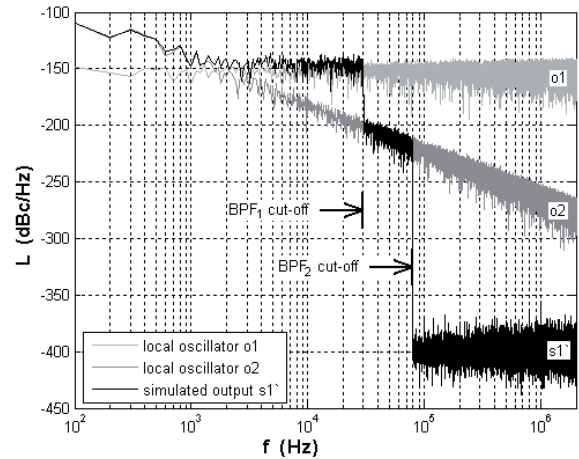

Fig. 9. The phase noise in the output signal s_1' of the system compared with oscillators O_1 and O_2 phase noise courses.

Low levels of the phase noise in Fig. 9 imply from initial model settings and they serve for an obvious expression of a coincidence between simulation results and theoretical presumptions. In our future work, real parameters are going to be used for the model adjustment.

6. Conclusion

The main focus of this paper is on the examination of the oscillators multiplicative phase noise influence in the space communication systems. Five basic noise processes are described asymptotically with a help of a power law. The simulation procedure for modeling the oscillator output signal degraded by the arbitrary phase noise is introduced. The verification of the proper disturbed signal generation is made in the time domain using three types of Allan variances. The validity is also checked by the asymptotic direct recalculation of the frequency domain phase noise to time domain Allan variances. A simple communication chain with two oscillators degraded by different phase noise courses is modeled. The influence of the phase noise combination on the useful signal is examined. All simulation results are in a good agreement with theoretical presumptions.

The basic model of the communication system will be extended. Our future work also counts with the presence of the additive thermal noise, which arises only on the receiver side of the system. Such an extended model is going to be utilized for the quantification of the influence of both noise types (additive thermal noise and multiplicative phase noise). Especially the cases of the long distant space communications, where the system bandwidth is decreased due to the useful energy absence, are going to be investigated.

Acknowledgements

References

[1] MARTIN, W. L., NGUYEN, T. M. *CCSDS – SFCG Efficient Modulation Methods Study – A Comparison of Modulation Schemes – Phase 1: Bandwidth Utilization.* Recommendation for space data system standards. CCSDS B20.0-Y, 1993.

[2] ŠPAČEK, J., KASAL, M. The low rate telemetry transmission simulator. *Radioegineering*, December 2007, vol. 16, no. 4, p. 24 to 31. ISSN 1210-2512.

[3] KASAL, M. *Frequency Synthesis in Communication Systems Experimental Satellites.* Brno: Vutium, 2005. 35 p. ISBN: 80-214-2982-8. (In Czech.)

[4] PETTAI, R. *Noise in Receiving Systems.* New York: Wiley-Interscience, 1984. 296 pages. ISBN 0471892351.

[5] HAJIMIRI, A., LEE, T. H. A General theory of phase noise in electrical oscillators. *IEEE Journal of Solid-State Circuits*, February 1998, vol. 33, no. 2, p. 179 – 194.

[6] HAJIMIRI, A., LEE, T. Oscillator phase noise: A tutorial. *IEEE Journal of Solid-State Circuits*. March 2000, vol. 35, no. 3, p.326 to 336.

[7] VASILESCU, G. *Electronic Noise and Interfering Signals: Principals and Aplications.* Berlin: Springer, 2005. 728 pages. ISBN 3540407413.

[8] CHANG, K. *Encyclopedia of RF and Microwave Engineering.* New Jersey: John Willey & Sons, 2005. ISBN 0-471-27053-9.

[9] KASAL, M. *Radio Rellay and Satellite Communication.* Lecture notes. Brno: MJ Servis, 2003. ISBN 80-214-2288-2. (In Czech.)

[10] RILEY, J. *Handbook of Frequency Stability Analysis.* Beaufort: Hamilton Technical Services, 2007. Available on web: http://www.stable32.com/Handbook.pdf.

[11] BAR-GUY, A. *Oscillator Phase Noise Model.* Matlab Central. An open exchange for the Matlab and Simulink user community. Available on web: http://www.mathworks.com/matlabcentral/fileexchange/8844.

[12] HOWE, D. A., ALLAN, D. W., BARNES, J. A. *Properties of Oscillator Signals and Measurement Methods.* NIST, Boulder, Colorado. Available on web: http://tf.nist.gov/phase/Properties/main.htm.

[13] LESAGE, P., AYI, T. Characterization of frequency stability: Analysis of the modified Allan variance and propertis of its estimate. *IEEE Transactions on Instrumentation and Measurement,* December 1984, vol. IM-33, no. 4, p. 332-336.

About Authors ...

Ondřej BARAN was born in Frýdek–Místek, Czech Republic, in 1983. He received his master's degree in Electrical Engineering from the Brno University of Technology in 2007. At present he is a PhD student at the Department of Radio Electronics, Brno University of Technology. His research interest is focused on the systems for space communications.

Miroslav KASAL (born in 1947 in Litomyšl, Czech Republic) graduated in communication engineering from the Faculty of Electrical Engineering, Brno University of Technology, in 1970. In 1984 he obtained his PhD degree in metering engineering. He was the head of the NMR Department and Electronics Laboratory of the Institute of Scientific Instruments, Academy of Science of the Czech Republic (1991 – 2002). Since 2002 he has been with the Department of Radio Engineering, Faculty of Electrical Engineering and Communication, Brno University of Technology, as professor. Dr. Kasal is a senior member of the IEEE. He has authored or coauthored a number of papers in scientific journals and conference proceedings. Dr. Kasal received the Award of the Rector of the Brno University of Technology, the SIEMENS Prize for research (2004), and the Prize of the Minister of Education of the Czech Republic for research (2007).